ELSEVIER

Journal of Nuclear Materials 281 (2000) 1–14

journal of nuclear materials

www.elsevier.nl/locate/jnucmat

Pressure building during the early stages of gas production in a radioactive waste repository

Bernard Bonin [a,*], Michel Colin [a], Anne Dutfoy [b]

[a] *IPSN, Département de PRotection de l'Environnement, Service d'Etudes et de Recherches sur la Géosphère et l'élimination des Déchets, Fonteray aux Roses, France*

[b] *EDF, Direction des Etudes et Recherches, Clamart, France*

Received 13 December 1999; accepted 19 June 2000

Abstract

In a radioactive waste repository, hydrogen may be produced by anoxic corrosion of the metallic components, and by water radiolysis. The design of deep geological repositories presently envisaged in many countries tends to inhibit the migration of every chemical species coming from the repository, by means of several concentric watertight barriers. This tightness, which is desirable for other reasons, might prevent hydrogen evacuation and cause a pressure rise in the near-field. Can this pressure break the barriers? In the first stage of the process, the hydrogen dissolves in the porewater. It is shown in the present paper that in the vicinity of a steel surface embedded in clay, the pressure rise due to the production of *dissolved* hydrogen may be large already (a few MPa), and may represent a significant fraction of the barrier resistance limit. In the second phase of the process, a gas bubble may form, causing a further pressure increase. The problem of gas production in geological repositories is treated here as a special case of thermo-hydro-chemico-mechanical coupling in a porous medium. The time needed for the bubble to form depends on the nature of the metal, and on the characteristics of the barrier. The purpose of this paper is to give orders of magnitude for the time and space scales associated with hydrogen production in the near-field of a deep repository, before the formation of a gaseous phase. The conditions under which a gas phase forms are also discussed.

1. Introduction

Is gas production in a radioactive waste repository a safety problem?

Several detrimental consequences of gas production can be envisaged [1–13]. The main concern is probably the damage to the engineered or geological barriers, due to an uncontrolled pressure rise.

The problem of gases in a radioactive waste repository depends essentially on the production rates, and on the capability of the barriers to evacuate them.

An abundant literature [14,15] exists on the mechanisms of gas generation (here, the term 'gas' is not used properly, since 'gas species' are firstly produced in dissolved form). Many studies have been devoted to the behaviour of a gas bubble in a repository [1,2,4, 6–9,11–13]. However, the first stage of the evolution of the system, in which the gas species are produced in dissolved form, has received little attention. This stage cannot be neglected, because in a deep geological repository, the very high hydrostatic pressure inhibits and delays the formation of a gas phase. The present paper is devoted mainly to the study of this first stage. The system modelled here is a simple planar interface between a saturated porous medium and a metal submitted to corrosion. We show that important effects due to hydrogen production can be expected in the vicinity of this interface, even in the absence of a gas bubble.

* Corresponding author. Present address: COGEMA, Direction de la Recherche et du Développement 2, rue Paul Dautier, BP 4 78141, Vélizy cedex, France. Tel.: +33-1 39 26 38 41; fax: +33-1 39 26 27 13.

E-mail address: bbonin@cogema.fr (B. Bonin).

0022-3115/00/$ - see front matter
PII: S0022-3115(00)00184-7

The problem of gas production in geological repositories can be viewed as a special case of thermo-hydro-chemico-mechanical coupling. It may also arise for other kinds of wastes, for which the gas tightness of landfill liners and the long-term integrity of the barriers could be an issue.

2. Mechanisms of gas generation

Several review papers exist on the mechanisms of gas generation [14,15]. We shall only summarize here the main conclusions.

The mechanisms which may a priori be envisaged for gas production in a radioactive waste repository are:

1. helium production due to the alpha activity of radioactive wastes,
2. water vaporization by heat generating wastes,
3. water radiolysis,
4. hydrogen production due to the corrosion of the metallic components in the repository,
5. microbial activity and degradation of organic matter.

Several gaseous species can be generated by these various mechanisms (He, H_2O, CO_2, H_2). However, it is generally agreed that in a deep radioactive waste repository for reprocessed or spent fuel, the main contributor is hydrogen from metallic corrosion [14–16]. The metal considered here can be the iron or steel from the canisters or from the 'sustainment structures'. The zirconium from the fuel cladding is not expected to contribute significantly to hydrogen production, since the corrosion rate of Zr alloys in water is extremely low.

The basic corrosion reaction is as follows:

$$M + H_2O \leftrightarrow MO + H_2. \quad (R1)$$

Several corrosion mechanisms exist, ranging from corrosion in etch pits (localized corrosion) to general corrosion (over the entire metallic surface). In the following, we shall consider only general corrosion, because this corrosion mode is expected to prevail in the reducing conditions met in a deep repository [17,18].

In this case, the relevant parameter which describes the gas production rate is the corrosion rate V_c (expressed in m/s or, more conveniently, in μm year^{-1}).

The hydrogen production rate j (in mol m^{-2} s^{-1}) is directly related to the corrosion rate V_c, via

$$j = \frac{\rho_m V_c}{M_m}, \quad (1)$$

where ρ_m is the metal density and M_m its atomic weight.

This equation assumes that 1 mole of hydrogen is produced per mole of consumed metal.

This hydrogen is produced, irrespective of the details of the corrosion mechanism.The rate evaluated via Eq. (1) is only an order of magnitude, since the actual stoichiometry may differ from the one sketched here by a factor of two according to the exact formula of the formed oxide (in this paper, the notation MO is taken as a generic notation for any metallic oxide).

The corrosion rate depends on many parameters, including the nature of the metal, the temperature and the redox and pH conditions in the porewater. Generally, the corrosion rate increases in acidic and saline conditions [17,19].

Also, the corrosion rate may depend on the hydrogen concentration in the porewater, slowing down as the concentration increases, and as the metal surface area available for corrosion decreases.

According to the neutral or basic pH and slightly reducing Eh conditions expected in the near-field of a deep repository, the most probable iron corrosion reactions are

$$Fe + 2H_2 \leftrightarrow Fe(OH)_2 + H_2 \uparrow \quad (R2)$$

and

$$3Fe + 4H_2O \leftrightarrow Fe_3O_4 + 4H_2 \uparrow. \quad (R3)$$

For both reactions, the hydrogen equilibrium concentration in the porewater is expected to be high [10,15,20].

As long as the hydrogen concentration stays far below this equilibrium value, the 'constant rate' hypothesis is valid. Anyway, the poor knowledge of the nature of the species formed by corrosion suggests that the constant rate hypothesis remains probably the best available assumption.

In the following, we shall consider mainly the anoxic, general corrosion of carbon or low-alloyed steel. Gas production is expected to be governed by corrosion of this kind of material because it is likely to be a major component of a repository, and because its corrosion rate is rather high.

Using the data provided by UK AEA, PNC and the CEN SCK [21–26], Gras proposed an analytical expression for the corrosion rate of carbon or low-alloyed steel in reducing conditions [21]:

$$V_c\ (\mu m\ year^{-1}) = 8200 \exp(-2435/T). \quad (2)$$

Orders of magnitude for the hydrogen production at ambient temperature are summarized in Table 1.

Table 1
Orders of magnitude for the hydrogen production at ambient temperature

Corrosion rate, V_c	3 μm year^{-1} (10^{-13} m s^{-1})
Hydrogen production rate, j	0.4 mol year^{-1} m^{-2} (1.2×10^{-8} mol s^{-1} m^{-2})

In the following, a constant corrosion rate will be assumed, with the order of magnitude given above. Further justification for this constant rate hypothesis can be found in the evaluation of the involved characteristic times.

3. Characteristic times

In this section, we try to locate the process of hydrogen release in the chronological sequence of the repository evolution.

3.1. Corrosion time

The hypothesis of constant corrosion rate makes it possible to determine the duration of the corrosion process: $t_c = e/V_c$, where e is the metal thickness. Assuming that e is between 5 and 20 cm (this range is supposed to be reasonable for a canister thickness), the above mentioned corrosion rate leads to a corrosion time t_c between 15 000 and 60 000 years.

3.2. Resaturation characteristic time

We make the hypothesis that the barrier has gone back to saturation before the beginning of the corrosion process. Three arguments justify this hypothesis:

1. the corrosion process needs water,
2. the resaturation time of a typical clay engineered barrier 1 m thick is of the order of hundred years [27]. This time is comparable to the thermal time, and shorter than the corrosion time of a typical steel canister 10 cm thick. Most of the corrosion thus occurs with a fully resaturated barrier, which has gone back to thermal equilibrium,
3. the hydrogen produced by metallic corrosion is an anoxic process. It can start only in reducing conditions, when all the air initially contained in the porous medium has disappeared.

3.3. Redox-flip characteristic time

Anoxic conditions prevail in deep geological repositories. Once the barrier is fully resaturated, the transition between oxidizing and reducing conditions is expected to be rapid, since the characteristic time for damping the oxidizing perturbation due to the excavation is generally supposed to be much shorter than the corrosion time, of the order of a few years or decades [28,29].

3.4. Thermal characteristic time

According to Eq. (2), corrosion rates depend on temperature [21]. The order of magnitude of the corrosion rate mentioned above is typical of 'ambient temperature' conditions. This choice of values may thus be questionable in the case of heat generating wastes. However, in the near-field the thermal characteristic time (a few hundred years) is usually small as compared with the corrosion time, so that most of the hydrogen production process takes place when the system is close to thermal equilibrium. This might not be true in the case of spent fuel, where the temperature rise is higher and lasts longer. Due to this 'low temperature assumption', we probably have a low estimate of the corrosion rate.

Given the orders of magnitude for these characteristic times, the modeling of the hydrogen release will start assuming a fully resaturated barrier, reducing conditions and ambient temperature. In these conditions, despite its crudeness, the constant rate hypothesis is probably a reasonable assumption.

4. Gas migration

In this section, we deal with the evolution of hydrogen in the medium.

Several stages can be distinguished in this evolution:

In the first stage, the hydrogen dissolves in the porewater, and migrates by advection and diffusion. Concentration and pressure already build up because the additional dissolved hydrogen cannot escape easily from the production zone.

In a second stage of the evolution, a gas phase may form if the hydrogen concentration becomes high enough (Fig. 1). The system then becomes two-phase flow, and the pressure buildup regime changes.

During stages I and II, the pressure buildup may lead to gas breakthrough or to the fracturation of the medium, with various degrees of damage to the barrier. This event should bring the system back to its initial hydrostatic pressure.

After all the metal has been consumed by the corrosion process, the hydrogen production stops, and a relaxation of the system takes place, with a resorption of all perturbations (stage III): if it has formed, the bubble itself then resorbs. A pressure relaxation occurs in the permeable compressible medium, together with a relaxation of the hydrogen concentration by diffusion and advection.

This evolution can be described in the diagram pore pressure P_h vs concentration of hydrogen dissolved in the porewater c at the metal–barrier interface (Fig. 2). The system is represented by a point, which moves with time in this diagram.

At the beginning of the production process ($t = 0$), the concentration of dissolved hydrogen in the porewater is $c = 0$, and P_h equals the pore pressure of the unperturbed system

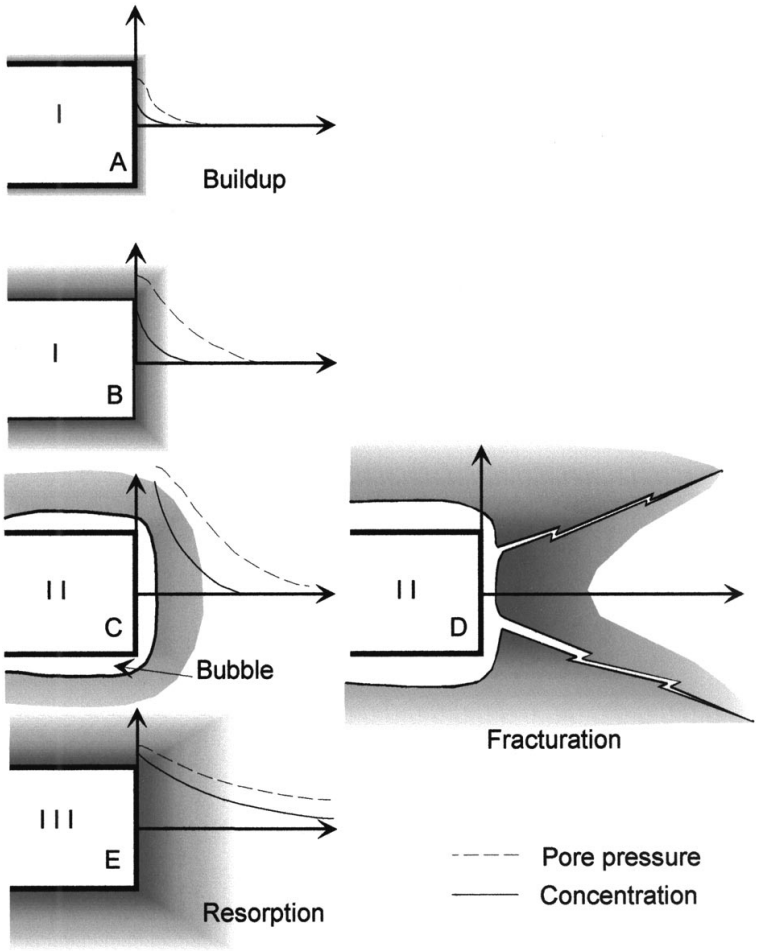

Fig. 1. System evolution.

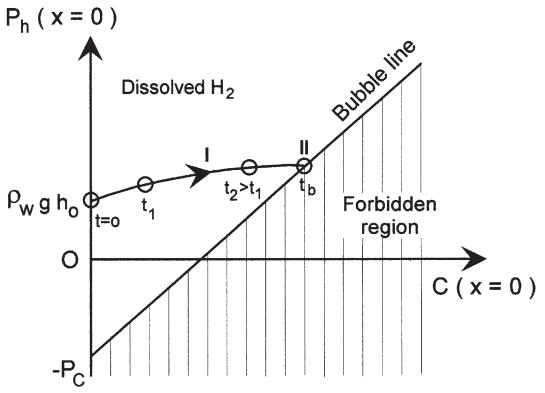

Fig. 2. System evolution in the diagram pressure vs concentration at the metal–barrier interface.

$$P_{\mathrm{h}} = \rho_w g h_0, \tag{3}$$

where ρ_{w} is the density of liquid water, g the gravity constant and h_0 the repository depth.

The concentration increases with time, causing an increase of the pore pressure. This increase of pore pressure will be small if the medium is very permeable or very compressible, and large in the opposite case.

Two conditions must be met for a gas phase to form:

(1) The pressure in the bubble must equal the pore pressure P_{h} plus the capillary pressure P_{c}

$$P_{\mathrm{b}} = P_{\mathrm{h}} + P_{\mathrm{c}}. \tag{4}$$

By writing this equation, we assume implicitly that a capillary pressure P_{c}, characteristic of the medium, can be defined. Strictly speaking, this is true only if the medium can be approximated by a capillary bundle with a sharply peaked pore size distribution. In this approximation, the suction P_{c} is associated with the departure

of free water from the medium, and is related to the pore size in the medium a and to the surface tension of the air–water interface σ via Jurin–Laplace law

$$P_c = 2\sigma/a. \tag{5}$$

This is of course a rough description of the real porous medium, where one usually finds a wide distribution of pore sizes. As defined here, the parameter P_c is only meant as an order of magnitude for the gas pressure needed to desaturate the medium.

(2) The hydrogen is supposed to be in chemical equilibrium between the gas phase and the aqueous phase

$$(H_2)\ \text{gas} \leftrightarrow (H_2)\ \text{dissolved}. \tag{R4}$$

This condition is expressed by Henry's law:

$$P_b = c/\kappa_H, \tag{6}$$

where κ_H is Henry's constant ($\kappa_H = 7.6 \times 10^{-6}$ mol Pa^{-1} m^{-3} for hydrogen at room temperature [33]) and c is the concentration of hydrogen dissolved in the porewater.

Elimination of the unknown P_b from Eqs. (5) and (6) yields

$$P_h = c/\kappa_H - P_c. \tag{7}$$

This expression defines a straight line in the diagram pore pressure P_h vs concentration c at the metal–barrier interface. If this line is met during the system evolution, a gas bubble forms (Fig. 2).

It should be noted that the solubility of hydrogen decreases with increasing temperature. Here again, the use of Henry's constant taken at room temperature is a very rough approximation.

We model the system evolution during stage I, taking into account simultaneously the hydrogen concentration and pore pressure in the porous medium. The purpose of this model is solely to extract the main orders of magnitude for the process considered here, as well as their time and length scales.

5. Mathematical description of stage I

The hydrogen is produced at the interface and migrates into the saturated, homogeneous, isotropic porous medium. The hydrogen concentration in the porewater $c(x, t)$ obeys the usual transport equation for non-interacting solutes [30]:

$$\frac{\partial c}{\partial t} = \frac{D_e}{\omega}\nabla^2 c + \frac{1}{\omega}\mathrm{div}\left(\frac{cK}{\rho_w g}\mathrm{grad}\ P_h\right), \tag{8}$$

where D_e is the effective diffusion constant for hydrogen diffusion in the porous medium, K is its saturated water permeability, ω its porosity and $P_h(x, t)$ the local pore pressure. Eq. (8) assumes that there is no well or source of hydrogen within the porous medium.

The system is closed by writing the equation describing the evolution of pore pressure. In the absence of a concentration gradient, the pore pressure would obey the usual piezometric equation in a permeable homogeneous compressible medium obeying Darcy's law

$$\frac{\partial P_h}{\partial t} = \mathrm{A}\nabla^2 P_h, \tag{9}$$

where the quantity A is the hydraulic diffusivity of the porous medium. Classically, A is given by $A = K/\Sigma_S$, where the permeability K and specific storage coefficient Σ_S have the typical values given in Table 2 for a clay and a sand [30].

A complementary term must be added to Eq. (9), to take into account the pressure variation due to a variation of hydrogen concentration

$$\frac{\partial P_h}{\partial t} = A\nabla^2 P_h + \frac{1}{\kappa}\frac{\partial c}{\partial t}. \tag{10}$$

Here, $1/\kappa$ is the rate of pressure increase due to a concentration increase in a fixed volume of porewater. We assume that this rate is about the same when all the hydrogen is dissolved and when part of it is in gas form, so that $1/\kappa$ is of order $1/\kappa_H$, the inverse of Henry's constant. This assumption is justified in Appendix A.

Eqs. (8) and (10) have two coupled variables, i.e., concentration c and pore pressure P_h. This system of coupled differential equations has been solved by standard numerical methods, e.g., by means of a finite difference homemade code, using the differential method, with explicit approximation, and constant time and space steps.

The chosen geometry is a simple infinite planar interface separating the metal submitted to corrosion and

Table 2
Typical hydraulic and transport parameters for a clay and a sand barrier

	Clay	Sand
Porosity, ω	0.2	0.3
Capillary pressure, P_c (MPa)	10	10^{-3}
Saturated permeability, K (m s^{-1})	10^{-12}	10^{-7}
Specific storage coefficient, Σ_S (m^{-1})	3×10^{-4}	3×10^{-4}
Hydraulic diffusivity, $A = K/\Sigma_S$ (m^2 s^{-1})	3×10^{-9}	3×10^{-4}
Effective diffusion constant for the concentration, D_e (m^2 s^{-1})	10^{-11}	6×10^{-10}

the permeable, compressible porous medium of the barrier. With this hypothesis, the problem becomes one-dimensional. Thanks to its simplicity, this geometry should yield orders of magnitude for the time and length scales of the processes considered here. This planar one-dimensional hypothesis will be appropriate if the length scale of the perturbation due to hydrogen release is short in comparison with the scale of an engineered barrier. An a posteriori justification for this assumption will be given below.

The boundary conditions are as follows:

$$(\text{grad } P_{\text{h}})_{x=0} = \frac{j}{K} g M_{\text{w}}. \tag{11}$$

This equation, where M_{W} is the molar mass of water, describes a 'well term' associated with the water consumption by the corrosion reaction. It assumes that the metal–barrier interface is immobile.

$$(\text{grad } c)_{x=0} = -\frac{j}{D_{\text{e}}}. \tag{12}$$

This equation describes a 'source term' associated with the hydrogen production by the corrosion reaction.

Initial conditions are as follows:

$$P_{\text{h}}(x, t=0) = \rho_{\text{w}} g h_0, \tag{13}$$

$$c(x, t=0) = 0. \tag{14}$$

These equations impose hydrostatic pressure and zero concentration everywhere at the beginning of the evolution.

Two calculations were made for a sand and a clay barrier, respectively. The corresponding *parameters* are given in Table 2.

It has been assumed here that the effective diffusion constant D_{e} for hydrogen in water is equal to the self-diffusion coefficient of water in the porous medium [5,31].

The results of the numerical calculation are as follows:

The hydrogen concentration and pore pressure at the interface increases with time. Initially, this increase is very rapid, and slows down after some time (Fig. 3).

The hydrogen concentration decreases with the distance to the interface. Initially, the concentration profile is confined close to the interface, and spreads out with time. In the case of clay for 5 years of evolution after the beginning of the corrosion reactions, the size L_{c} of the zone invaded by dissolved hydrogen (defined at half maximum of the concentration profile curve) is only 10 cm (Table 3).

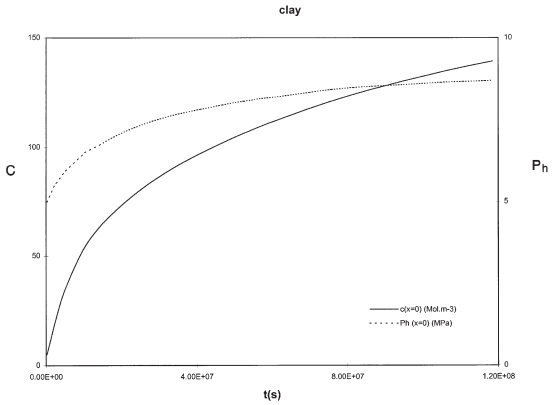

Fig. 3. Time evolution of the concentration c and pore pressure P_{h} at the metal–barrier interface. Case of a clay barrier.

Table 3
Results of the system evolution at the onset of bubble formation for a clay and a sand barrier, assuming a corrosion rate of 3 μm/year in a repository located at a depth of 500 m

	Clay	Sand
Bubble time t_b (years)		
Numerical estimate	4.1	46
Analytical approximation Eq. (18)	6.0	46
Pore pressure at the interface $P_h(x=0,\ t=t_b)$ (MPa)		
Numerical estimate	8.7 (overpressure = 3.7)	5 (overpressure ≈ 0)
Analytical approximation Eq. (19)	7.2 (overpressure = 2.2)	5 (overpressure ≈ 0)
Hydrogen concentration at the interface $c(x=0,\ t=t_b)$ ($mol\ m^{-3}$)		
Numerical estimate	139	43
Analytical approximation Eq. (20)	148	43
Size of the zone invaded by dissolved hydrogen L_c (m)		
Numerical estimate (width at half maximum)	0.10	1.6
Analytical approximation Eq. (21)	0.10	1.6
Size of the zone affected by hydraulic perturbation L_h (m)		
Numerical estimate (width at half maximum)	0.60	650
Analytical approximation Eq. (22)	0.70	650

The pore pressure profile also decreases with the distance to the interface, and spreads out with time. The size L_h of the zone affected by the hydraulic perturbation is about 60 cm for clay after 5 years (Table 3, Fig. 4).

These evolutions can be displayed in the P_h–c diagram at the metal–barrier interface (Fig. 5). With the parameters given above, the curve, which represents the system evolution, is close to a straight line. In the case of sand, the slope of this curve is nearly zero because this medium is very permeable and evacuates any pressure increase readily. In all practical cases, this slope is smaller than the slope of the bubble line

$$\frac{dP_h}{dc} = \frac{1}{\kappa_H} \tag{15}$$

so the curve can meet the bubble line.

A bubble will form if the hydrogen production does not stop before the bubble line is reached, i.e., if there is enough metal available for corrosion.

This 'bubble time' is about 5 years for clay and 50 years for sand, assuming a typical corrosion rate of 3 μm year^{-1} and a repository located at a depth of 500 m.

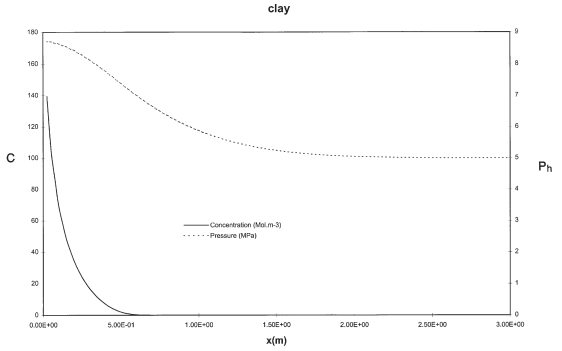

Fig. 4. Spatial distribution of the concentration and pore pressure after 500 years of hydrogen production. Case of a clay barrier.

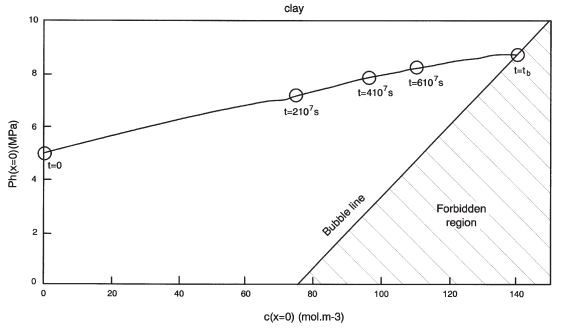

Fig. 5. System evolution in the diagram pressure vs concentration at the metal–barrier interface. Case of a clay barrier.

With this corrosion rate, the time t_b is much shorter than the corrosion time t_c mentioned previously. It is thus possible to conclude that advection–diffusion through the barrier cannot prevent the formation of a bubble, in clay as well as in sand. However, it should be noted that the bubble time t_b depends strongly on the hydrogen production rate j and on the repository depth h_0. If j is smaller than the nominal value assumed here, the formation of a bubble might be delayed considerably (Fig. 6).

With such short bubble times and small characteristic lengths, it is plausible that diffusive transport of hydrogen dominates over advective transport. If the advective term is neglected in the transport equation Eq. (8), the following expressions hold for the pore pressure and hydrogen concentration at the interface:

$$P_h(x=0,t) = \rho_w g h_0 + \frac{2}{\sqrt{\pi}} \frac{j}{\omega \kappa_H} \frac{1}{1+\sqrt{D_e/\omega A}} \sqrt{\frac{t}{A}}, \tag{16}$$

$$c(x=0,t) = \frac{2}{\sqrt{\pi}} j \sqrt{\frac{t}{\omega D_e}}. \tag{17}$$

The time t_b taken for a bubble to form is then

$$t_b = \frac{\pi}{4}\left[\frac{\omega \kappa_H (\rho_w g h_0 + P_c)}{j\left(\sqrt{\frac{\omega}{D_e}} - \sqrt{\frac{1}{A}}\right)}\right]^2. \tag{18}$$

At the onset of bubble formation, the pore pressure reached at the metal surface is approximately

$$P_h(x=0, t=t_b) = \frac{\rho_w g h_0 + P_c \sqrt{\frac{D_e}{A\omega}}}{1-\sqrt{\frac{D_e}{A\omega}}} \tag{19}$$

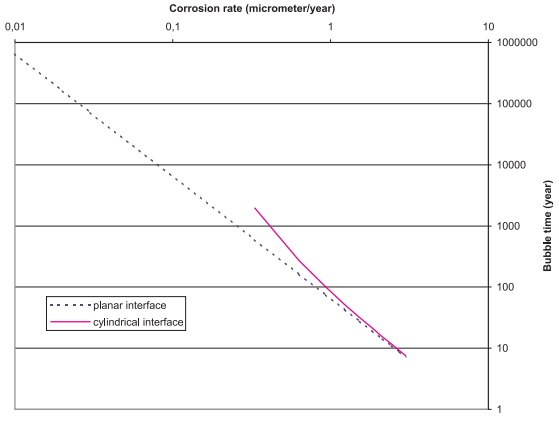

Fig. 6. Bubble time vs corrosion rate for a planar interface and a cylindrical interface of radius 50 cm. Case of a clay barrier.

and the concentration at the interface is

$$c(x=0,t=t_b)=\kappa_H\frac{\rho_w g h_0+P_c}{1-\sqrt{\frac{D_e}{A\omega}}}. \quad (20)$$

In this approximation, the characteristic size of the zone invaded by dissolved hydrogen after time t is

$$L_c=\sqrt{D_e t/\omega} \quad (21)$$

and the characteristic size of the zone affected by the hydraulic perturbation is

$$L_h=\sqrt{A t}. \quad (22)$$

In the present case, these diffusion lengths correspond roughly to the width at half maximum of the concentration or pressure profile curves.

Results of the system evolution at the onset of bubble formation for a clay and a sand barrier are summarized in Table 3.

Note that for a clay barrier, the length scales evaluated above are short in comparison with the scale of an engineered barrier. This justifies a posteriori the planar one-dimensional hypothesis made in the mathematical description of the system. With a smaller corrosion rate, the hypothesis would lose its validity. It would then become appropriate to model an axisymmetric system with a finite canister radius, but the problem would lose somewhat in simplicity. With these restrictions in mind, we calculated the bubble time as a function of corrosion rate for a canister with 0.5 m radius (Fig. 6). As expected, the bubble time increases very sharply with decreasing corrosion rate. This increase is roughly proportional to V_c^{-2} for a planar interface. For a cylindrical interface, the time needed for a bubble to form is even longer, and becomes virtually infinite (larger than 100 000 years) for corrosion rates smaller than 0.1 μm year^{-1}.

6. Discussion

In the model described above, it has been assumed that the hydrogen produced by corrosion cannot disappear by reaction with the minerals from the barrier. Batch experiments on slurries of Boom clay did show that the reaction capacity for fresh clay is very small (1.2 mg H_2 per kg of clay [9]). However, this hypothesis may be questionable, as some minerals like gypsum and goethite might react with hydrogen [32].

We also assumed that the metal does not absorb the hydrogen produced by the corrosion reaction. Hydrogen is known to diffuse easily through metal matrices, and this might a priori lead to the introduction of a 'well' term in Eq. (2). This effect might delay or prevent pore pressure rise and bubble formation in the porous medium. However, a numerical evaluation show that the pore pressure rise and bubble formation are not significantly delayed if hydrogen incorporation into the metal is taken into account (see Appendix B).

In the model described above, it has been assumed that the interface between the metal and the porous medium is immobile, i.e., that the metal M and its oxide MO occupy the same volume. However, it is known that usually, MO occupies a larger volume than M [33]. If the metal is iron, the wustite FeO, the hematite Fe_2O_3, the magnetite Fe_3O_4 occupy a volume about twice the volume of the original metal. For the goethite FeOOH, this factor is about 4. It is technically possible to incorporate the volume increase between the metal and its oxide into the model by modifying the boundary condition Eq. (11), which would then become

$$(\text{grad } P_h)_{x=0}=\frac{j}{K}\rho_w g\left(\frac{M_w}{\rho_w}+\frac{M_m}{\rho_m}-\frac{M_{MO}}{\rho_{MO}}\right), \quad (23)$$

but the results are quite insensitive to this improvement. This is why we neglected it in the following.

7. Second stage

At this stage, a gas phase forms at the metal surface. Most of the studies already published on gas migration from repositories [1–13,34] deal in fact exclusively with this second stage, and describe the bubble evolution by use of the two-phase flow theory in porous media [35]. In this paper, no attempt was made to model the system evolution after the onset of bubble formation, because of several difficulties

(1) During stage II, the length scale of the hydraulic perturbation becomes comparable or larger than the scale of the engineered barrier. A one-dimensional approach then becomes inadequate, and the full geometry of the repository must be taken into account.

(2) Can the corrosion reaction be maintained if a bubble is present? The bubble itself might inhibit the arrival of water to the metal surface, and thereby stop the hydrogen production. In this hypothesis, the bubble would resorb as soon as it is formed!

Moreover, the upward travel distance of the bubble during the corrosion time t_c may not be small in comparison to the typical vertical extension of the canister, so the bubble cannot be considered as immobile during stage II, even in clay. This brings severe complications to the description of the system evolution in stage II.

(3) According to several studies, the gas–liquid interface is probably unstable in clay barriers, due to the influence of viscous and capillary forces [36,37]. The shape of the bubble is thus expected to be quite complicated. The assumption of a planar gas–liquid interface

being probably inadequate, this hampers the modelling of the system.

(4) In a compact clay, the major part of the pore-water is adsorbed onto clay minerals, and is very difficult to displace by gas injection. The application of standard two-phase flow theory to such materials is very questionable [5,9].

Altogether, a detailed description of this phase is beyond the scope of this paper.

8. Gas breakthrough

It should be noted that a real barrier is not perfectly homogeneous, and that the capillary barrier has not the same height P_c everywhere. The conditions for nucleation of a gas phase will be met earlier in the largest pores of the medium, where P_c is lowest. The bubble time evaluated above for a hypothetical homogeneous medium should therefore be viewed as an upper limit.

Gas breakthrough experiments through argillaceous media have been conducted by several researchers, both on samples and in situ [7–9,38–44]. They indicate that breakthrough might occur for moderate overpressures, of the order of 1–10 MPa for consolidated clay, and is roughly equal to the sum of the swelling pressure and the hydrostatic pressure in the barrier. This breakthrough pressure lies in the same range as the overpressure already reached in the clay barrier at the end of stage I. This breakthrough does not seem to be accompanied by the desaturation of an important volume of the barrier. After breakthrough, the barrier often recovers more or less totally its confinement properties. This suggests that breakthrough could be associated with preferential pathways, where the capillary barrier is lowest. The pressurized gas does not penetrate uniformly through clay, but makes its way through a very small number of passages [5,9,38–44], probably the ones formed by the percolation of the largest pores, with a depressed capillary barrier. Due to the very high suction in clay, most of its volume will remain 100% water-saturated during gas breakthrough.

Finally, can gas breakthrough be an effective mode of pressure release in the near-field?

Gas breakthrough experiments on samples and in situ often yield different results [9]. The low breakthrough pressure measured in in situ experiments can be attributed to large-scale inhomogeneities in the medium, or to the existence of a disturbed zone around the injection boreholes. Little is known about these scale effects. Significant overpressure (larger than 1 MPa in many cases) is often found in natural underground environments and has obviously been maintained during very large periods of time [45]. The mere fact that natural underground gas pockets exist indicates that capillary gas breakthrough does not necessarily operate efficiently in all cases.

9. Fracturation of the barrier

Capillary breakthrough is not the only mechanism of pressure release in the near-field. A hydraulic fracturation of the barrier can also occur, with detrimental consequences on the barrier integrity. Hydraulic fracturation sets an upper limit on the value of the pore pressure that can be accepted in the near-field.

The pore pressure can be compared to the typical resistance limit of the barrier. In a realistic, three-dimensional geometry, the stress field around the repository is rather complicated, and depends on the shape of the excavation and on the long-term mechanical properties of the components in the near-field. However, the planar, semi-infinite geometry assumed above brings a drastic simplification of the stress field. Furthermore, we assume that the porous skeleton of the barrier is a simple pileup of grains of density ρ_r, with no 'glue' in between, compacted by the lithostatic pressure

$$P_{\text{litho}} = \rho_r g h_0. \tag{24}$$

In this approximation, the barrier has no traction resistance, and will break when the pore pressure becomes larger than the lithostatic pressure (Fig. 7). In the absence of a bubble, the criterion for the breakup of the barrier is therefore

$$P_h = P_{\text{litho}}, \tag{25}$$

or, if a bubble has formed

$$P_{\text{gas}} = P_{\text{litho}} + P_c. \tag{26}$$

In fact, the two above conditions are strictly equivalent, since $P_{\text{gas}} = P_h + P_c$.

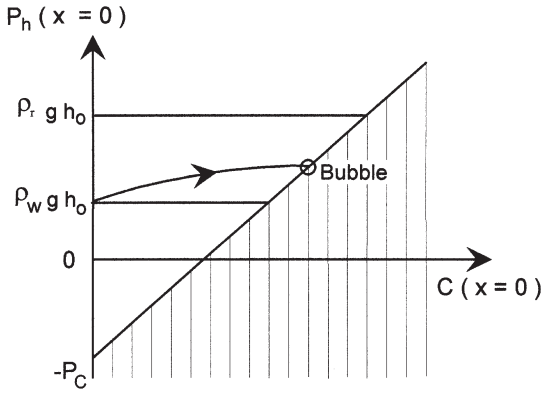

Fig. 7. System evolution. Comparison with the barrier resistance limits.

Despite their crudeness, it is hoped that the above hypotheses give the correct order of magnitude for the resistance limit of the barrier. For a typical repository located at a depth of 500 m, the lithostatic pressure is between 10 and 15 MPa. It has been shown above that the pore overpressure induced in the near-field by the production of dissolved hydrogen may be large already (a few MPa, for a clay barrier), but is probably not sufficient to break the barrier, as this pressure is only a fraction of the resistance limit evaluated above. If a bubble forms (stage II), the pressure increases further. A complete evaluation of the pressure reached in this second stage would be difficult, and is outside the scope of this paper. However, this stage II starts with an initially large overpressure in the near-field, so that it can be said that there is a very definite risk of barrier fracturation if clay barriers are used.

The depth h_0 of the repository is an important parameter in this issue of barrier fracturation. An increase of h_0 has two consequences. First, the pore pressure needed to break the barrier becomes larger as the lithostatic pressure P_{lith} increases. Second, as has been shown above, the bubble formation is inhibited and delayed by an increase of h_0 (t_b depends strongly on h_0, cf. Eq. (18)).

Both factors contribute to improving the safety of deeper repositories, as compared to shallower ones (Fig. 8).

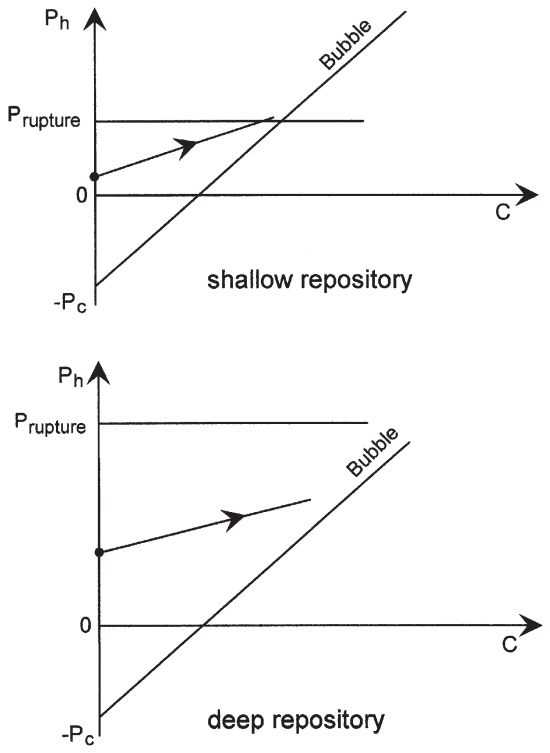

Fig. 8. Influence of depth. Comparison of the system evolution in a shallow and in a deep repository.

10. Conclusion

The problem of gas generation in a deep waste repository, viewed as a special case of thermo-hydro-chemico-mechanical coupling, has been treated in a rather crude way. In fact, the only coupling explicitly taken into account here is the hydro–chemical coupling, with the simplifying assumption of a constant reaction rate. The influence of the temperature has been neglected. Also, the mechanical consequences on the barrier have been simply deduced from the hydro-chemical evolution of the system.

With these assumptions, evolution of the system in stage I, i.e., before the formation of a gas phase, can be modeled in a very simple way. Hydrogen production at the metal–barrier interface causes the progression of two overlapping zones inside the barrier. The first one is 'contaminated' with dissolved hydrogen, and the second one is characterized by a perturbed pore pressure. The hydraulically perturbed zone extends further and faster than the contaminated zone, but is limited to less than one meter in the case of a clay barrier after five years evolution.

It is confirmed here that the transport capabilities of dissolved gas through clay barriers are very limited. With the parameters used in the present study (corrosion of carbon steel), the bubble forms within a few years in a clay barrier.

Before bubble formation, the magnitude of the pressure rise depends on the characteristics of the porous medium. Assuming typical values for the corrosion rate, the pressure increase ranges between zero (for a very permeable medium like sand) and a few MPa (for compacted clay). Although it is already non-negligible, this order of magnitude is smaller than the lithostatic pressure at the depth usually envisaged for deep geological disposal of wastes (10–15 MPa). Consequently, one does not expect a hydraulic fracturation of the barriers during the first stage of the system evolution. However, as can be seen from the orders of magnitude given above, the security margin is not large, and can be narrowed further by a decrease of the repository depth.

The use of a tight engineered barrier with strong capillary behaviour might have several adverse consequences:

- the formation of a gas bubble is accelerated, as compared to more porous media (Table 3),
- the pore pressure increases strongly, due to a high concentration of dissolved hydrogen in the near-field,
- hydrogen embrittlement of the corroding metal might also occur, with detrimental consequences on the mechanical characteristics of the canisters (Appendix C).

Once a bubble is formed, the pressure increase might be even more rapid, but this evolution is much more difficult to predict than when all the hydrogen is dissolved. For these reasons, it will certainly be easier to demonstrate the safety of disposal concepts designed to avoid the formation of a gaseous phase. Is it possible to reach this goal? Gas production by the waste is a near-field problem. In the design of the engineered barrier, a reasonable compromise has to be found between the tightness, required for a satisfactory waste confinement, and the permeability needed for a peaceful exit of the hydrogen produced by the corrosion process. Altogether, if bubble formation is to be avoided, special care must be devoted to the following key parameters: the corrosion rate, the amount of metal available for corrosion, the hydraulic and transport properties of the porous medium and the depth of the disposal facility.

The main uncertainty in the prevision of the system evolution comes from a poor knowledge of the metal corrosion rate in in situ conditions. Further studies on this crucial issue are urgently needed.

The above evaluation shows that even by giving extreme values to all important parameters, it is hard to avoid the formation of a hydrogen bubble if carbon steel is used in a clay barrier. However, the time taken for a bubble to form increases sharply with decreasing corrosion rate, and becomes virtually infinite for corrosion rates lower than 0.1 μm $year^{-1}$. This might be another incentive to consider seriously the use of low corrosion materials in a repository.

The metal of the container may not be the only or the main metallic source in the repository. Sustainment structures should also be considered, as they may involve large quantities of metal.

Avoiding the formation of a bubble might be more difficult for spent fuel than for retreated waste, because of the big casks, with much metal, and also because of the more severe heating, which will increase the corrosion rate and reduce the solubility of hydrogen.

Finally, the main contribution of the present paper is to show that important effects due to hydrogen production at the clay–metal interface can be expected in a waste repository, even before bubble formation. Due to the numerous uncertainties in the analysis, this question will probably deserve further investigation.

Acknowledgements

The authors sincerely thank F. Besnus, J. M. Gras and J. M. Peres, for providing useful documentation, M. Guillopé and G. Santarini for private communications on corrosion data, and C. Ferry, D. Stammose, C. Belot, A. Genty, T. Lassabatère, C. Gallé, O. Didry and S. Maillard for helpful discussions.

Appendix A. Evaluation of the rate of pressure increase due to a concentration increase in a fixed volume of water

We argue here that the inverse of Henry's constant κ_H can be seen as the rate of pressure increase due to the introduction of additional *dissolved* hydrogen in a constant volume of water, and that this interpretation can be kept below the bubble line.

In a diphasic system (liquid + gas), this rate is known

$$\frac{\partial P}{\partial c} = \frac{1}{\kappa_H}. \tag{A.1}$$

It is independent of the bubble volume, and should thus be the same when the bubble vanishes. This argument of continuity already suggests that the rate $\partial P/\partial c$ should be close to its value $1/\kappa_H$ if the system stays close to the bubble line.

Furthermore, when all the hydrogen is dissolved (no bubble), the rate $\partial P/\partial c$ can be evaluated as a function of the effective volume v of the hydrogen molecule in a fixed volume of liquid water

$$\partial P/\partial c = N_A v \alpha, \tag{A.2}$$

where N_A is Avogadro's number, and α is the water incompressibility $\alpha \equiv -V(\partial P/\partial V) \approx 2.2 \times 10^9$ Pa [33].

All common molecules which do not react chemically with water, like H_2, O_2, N_2, He, Ne, are expected to occupy an effective volume v of 'atomic' or 'molecular' size, of the order of 10^{-28} m^3. Eq. (A.2) then gives a rate of pressure increase $\partial P/\partial c \approx 10^5$ Pa m^3 mol^{-1} and indeed, for all these gases the inverse of Henry's constant $1/\kappa_H$ is numerically close to this value.

The above arguments corroborate this somewhat unorthodox interpretation of Henry's constant, and justify the assumption that $\partial P/\partial c$ should be close to $1/\kappa_H$, even in a monophasic system rather far from the bubble line.

Appendix B. Hydrogen absorption in the metal

We argue here that hydrogen absorption in the metal can be neglected in the description of the evolution of the hydrogen concentration and pore pressure fields in clay close to a clay–steel interface.

An abundant literature exists on solubility and diffusivity of hydrogen in steel [46–48].

Hydrogen in steel is monoatomic. A dissociation of the hydrogen molecule thus occurs at the metal surface

H_2	$\leftrightarrow$	2H
↑		↑
Dissolved in water		Dissolved in metal

Thermodynamic equilibrium between both phases at the metal surface can be expressed as

$$c_m^2(x=0) = \chi c(x=0), \tag{B.1}$$

where c is the dihydrogen concentration in the porewater and c_m the monohydrogen concentration in the metal.

χ is a constant which depends only on the metal nature and on temperature. Numerical values for χ are not directly available from the literature, but χ can be derived from the knowledge of Henry's constant κ_H and of Sievert's constant κ_S relating the hydrogen partial pressure P and the hydrogen concentration in porewater and in metal at thermodynamic equilibrium

$$P = c/\kappa_H = c_m^2/\kappa_S. \tag{B.2}$$

Hence

$$\chi = \kappa_S/\kappa_H. \tag{B.3}$$

Values of the Sievert's constant are quite different for ferritic–martensitic (body-centered) steel and for austenitic (cubic face-centered) steel. A compilation of values given in the literature for κ_S and κ_H gives the following order of magnitude for χ at ambient temperature (Table 4 [48]).

The hydrogen diffusion constant in the metal D_m also depends on the metal nature, and on its crystalline state. Typical values for steel at ambient temperature are also given in Table 4 [48].

The hydrogen produced by the corrosion reaction at the metal surface can diffuse both in the metal or in the porewater. In the approximation of purely diffusive transport of hydrogen in the porous medium near the surface, the dihydrogen production rate is given by Fick's law

$$j = D_e|(\text{grad } c)(x=0)| + \frac{D_m}{2}|(\text{grad } c_m)(x=0)|. \tag{B.4}$$

After time t, the characteristic diffusion length in the porous medium is

$$L_c = \sqrt{D_e t/\omega} \tag{21}$$

and the characteristic diffusion length in the metal is

$$L_m = \sqrt{D_m t}. \tag{B.5}$$

Table 4
Diffusion coefficient and partition coefficient for hydrogen in steel

	D_m ($m^2\ s^{-1}$)	χ ($m^3\ mol^{-1}$)
Bc steels (e.g., carbon steels)	10^{-11}–10^{-8}	8×10^{-5}–8×10^{-2}
Cfc steels (e.g., stainless steels)	10^{-16}–10^{-14}	8–80

The concentration gradients at the interface are thus of order

$$\text{grad } c(x=0) \approx \frac{c(x=0)}{\sqrt{D_e t/\omega}}, \tag{B.6}$$

$$\text{grad } c_m(x=0) \approx \frac{c_m(x=0)}{\sqrt{D_m t}}. \tag{B.7}$$

The hydrogen production rate can then be written as

$$j = \sqrt{\frac{\omega D_e}{t}} c(x=0) + \frac{1}{2}\sqrt{\frac{\chi D_m}{t}}\sqrt{c(x=0)}. \tag{B.8}$$

This equation gives the time evolution of the hydrogen concentration in the porewater at the interface.

The first term corresponds to hydrogen diffusion in the porewater, and the second one corresponds to hydrogen diffusion in the metal. This second term is dominant early in the evolution of the system (the concentration at the interface then grows proportional to time, as most of the hydrogen enters into the metal), whereas the first term takes over later (the concentration at the interface then grows proportional to the square root of time, as hydrogen practically no longer enters into the metal).

The transition between the two regimes occurs when both terms have the same magnitude. This occurs around time

$$t_m = \frac{1}{4}\frac{\chi^2 D_m^2}{j^2 \omega D_e}. \tag{B.9}$$

Using values for χ and D_m given in Table 4, the numerical evaluation of t_m in the case of a clay–steel interface at ambient temperature shows that t_m is smaller than a few months, regardless of the kind of steel under consideration. For $t \gg t_m$, hydrogen absorption into the metal becomes negligible and the system evolves as described in the body of the text.

The smallness of t_m in most practical cases justifies our statement that hydrogen absorption in the metal does not perturb significantly the evolution of the hydrogen concentration and pore pressure fields in the clay barrier.

Appendix C. Steel embrittlement due to hydrogen absorption

We argue here that hydrogen absorption in steel may cause embrittlement.

As discussed in Appendix B, the relationship between hydrogen concentration in the porewater and in the metal close to the surface can be written:

$$c_m^2(x=0) = \chi c(x=0).$$

Numerical values for χ are given in Table 4. With the typical parameter values chosen in the text for a clay–steel interface, it has been demonstrated above that the hydrogen concentration in the porewater at the bubble point is about $c(x=0)=130$ mol m^{-3}. For ferritic or martensitic steel, this corresponds to a hydrogen concentration in the metal c_m between 2×10^{-1} and 8 mol m^{-3}.

The critical concentration for embrittlement in this kind of steel lies in the range $c_m \approx 0.4$–40 mol m^{-3} [49,50]. The lower values are for steels with high mechanical characteristics (martensitic steel), whereas the higher values are for ferritic steel.

Given the above mentioned values, the eventuality of steel embrittlement by hydrogen incorporation during the corrosion process cannot be excluded.

References

[1] OECD, Near-field assessment of repositories for low and medium level radioactive waste, NEA NAGRA Workshop Proceedings, Baden, Switzerland, 23–25 November 1987, (1988) pp. 14–18.

[2] M.A. Jones, Gas generation in deep radioactive waste repositories; a review of processes, controls and models, DOE report DOE/HMIP/RR/90/086, 1990.

[3] F. Besnus and S. Voinis, in: Proceedings of the XIII International Symposium on the Scientific basis for Nuclear Waste Management, vol. 212, MRS'90 26–29 November 1990, Boston, USA, 1991, p. 901.

[4] W.R. Rodwell, P.J. Nash, Mechanisms and modelling of gas migration from deep radioactive waste repositories, NIREX Safety Studies Rept NSS/R250, 1992.

[5] S.T. Horseman, J.J.W. Higgo, J. Alexander, J. Harrington, Basic concepts and mechanisms of water, gas and solute movement in argillaceous media, British Geological Survey Technical Report WE/95/8C, 1995.

[6] B. Haijtink, T. Mc Menamin. Project on the effects of gas in underground storage facilities for radioactive waste, PEGASUS Project Proceedings of the progreess meetings held in Brussels (Belgium) June 1992, Report EUR 14816 EN, 1993, Cologne (Germany) June 1993, Report EUR 15734 EN, 1994, Rapolano Terme (Italy) June 1995, Report EUR 16746 EN, 1996.

[7] G. Volckaert, P. Grindrod, M. Impey, V. Fioravante, S. Horseman, Modelling and experiments on gas migration in argillaceous host rocks, AEN/ANDRA Workshop, Aix en Provence, France, September 1991 pp. 405–416 (1992).

[8] G. Volckaert et al. Modelling and experiments on gas migration in argillaceous host rocks, Final Report of the MEGAS project, EUR 16235 EN, 1995, 447 pp.

[9] L. Ortiz et al. Modelling and experiments on gas migration in repository host rocks European Commission, Nuclear Science and Technology, EUR 17453 EN, Final Report Phase 2, 1997, 155 pp.

[10] I. Neretnieks, Some aspects of the use of iron canisters in deep-lying repositories for nuclear waste, NAGRA Technical Report 85-35, 1985.

[11] I. Neretnieks, OECD, Gas generation and release from radioactive waste repositories, NEA/ANDRA Workshop Proceedings, Aix-en Provence, France, 1991, pp. 11–18 (1992).

[12] T. Manaï, EVEGAS, European validation exercise of GAS migration models through geological media, European Commission, Nuclear Science and Technology EUR 16639 EN, 1995.

[13] T. Manaï, Gas pressure buildup in a radioactive waste disposal repositories: hydraulic and mechanical effects. European Commission, Nuclear Science and Technology, EUR16753EN, 1996.

[14] V. Codazzi, Production d'hydrogène au cours du stockage de déchets radioactifs, CEA Technical Report, SCECF 297, 1993, 26 p.

[15] M. Rodrigo Minguez, Analysis of gas generation mechanisms in underground radioactive waste repositories (PEGASE Project) ENRESA Technical Publication 08/95, 1995.

[16] D.A. Lever, J.H. Rees, Gas generation and migration in waste repositories, in Ref. [1], 1988, p. 115.

[17] M. Pourbaix, Application de l'électrochimie à la science de la corrosion et en pratique, RT 204, Centre Belge d'Etude de la Corrosion, Bruxelles, 1972.

[18] J.M. Gras, Résistance à la corrosion des matériaux de conteneur envisagés pour le stockage profond des déchets nucléaires, EDF Technical Note HT 40/96/002/A (1996), Pourbaix, cf. Ref. [5].

[19] J.P. Simpson and R. Schenk, Corrosion induced hydrogen evolution on high level waste overpack materials in synthetic groundwaters and chloride solutions, Material Research Society Symposium Proceedings, vol. 127, 1989.

[20] M. Wiborgh, L.O. Hoglund, K. Prers, Gas formation in a type B repository and gas transport in the host rock, NAGRA report NTB 85-17, 1985.

[21] J.M. Gras, Résistance à la corrosion des matériaux de conteneur envisagés pour le stockage profond des déchets nucléaires, Note EDF/DER/SRNE, HT-40/96/002/A, 1996, 87 pp.

[22] G.P. Marsh, in: Proceedings of XIth International Symposium on the Scientific Basis for Nuclear Waste Management, vol. 112, MRS'87, November 1987, Boston, USA, (1988) pp. 85–97.

[23] W. Debruyn, H. Tas, J. Dresselaers, in: Proceedings of XI International Symposium on the Scientific Basis for Nuclear Waste Management, vol. 127, MRS'88, Berlin, Germany, (1989) p. 381.

[24] G.P. Marsh, K.J. Taylor, S. Sharland, A.J. Diver, Corrosion of carbon steel for the geological disposal of radioactive waste, CEC report, EUR-13671 EN, 1991.

[25] H. Ishikawa, A. Honda, N. Sasaki, Long life prediction of carbon steel overpack for geological isolation of radioactive waste, in: Proceedings of NACE Conference on Life Prediction of Corrodible Structure, Houston, 1991.

[26] A. Honda, N. Taniguchi, H. Ishikawa, A modelling study for long-term life prediction of carbon steel overpack for geological isolation of high level radioactive waste, in: Proceeding of the International Symposium on Plant Ageing and Life Prediction of Corrodible Structures, Sapporo, 1995.

[27] G. Thouvenin, A. Giraud, F. Homand, O. Didry, P. Hornet, T. Lassabatère, Numerical investigation of the hydration of a clay barrier: linear and non-linear approaches, in: Proceedings of the Fourth International Workshop on Key Issues in Waste Isolation Research, Barcelona, Décember 1998.
[28] M.A. Jones, Gas generation in deep radioactive waste repositories: a review of processes, controls and models, UKDoE report no. DoE/HMIP/RR/90/086, 1990.
[29] S.M. Sharland, P.W. Tasker and C.J. Tweed, The evolution of Eh in the porewater of a model nuclear waste repository, AERE-R12442, 1986.
[30] G. deMarsily, Quantitative Hydrogeology. Groundwater Hydrology for Engineers, Academic Press, New York, 1986.
[31] I. Neretnieks Diffusivities of some dissolved constituents in compacted wet bentonite clay and the impact on radionuclide migration in the buffer, Swedish Nuclear Fuel Supply Co. KBS Technical Report TR 82-27, 1982.
[32] L. Trottignon, M. Cranga, private communication.
[33] R.C. Weast (Ed.), Handbook of Chemistry and Physics, CRC, Boca Raton, FL, 1975.
[34] S. Mishra and P. Zuidema, Modelling gas migration from a low/intermediate level nuclear waste repository, in Ref. [11].
[35] P.G. de Gennes, Physico-chem. Hydrodynam. 4 (2) (1983) 175.
[36] M.C. Leverett, AIME Trans. 142 (1941) 152.
[37] R. Lenormand, E. Touboul, C. Zarcone, J. Fluid Mech. 189 (1988) 165.
[38] R. Pusch, T. Forsberg, Gas migration through bentonite clay, SKBF-KBS Technical Report 83-71, 1983, 15 p.
[39] R. Pusch, L. Ranhagen, K. Nilsson, Gas migration through MX-80 bentonite, Final report. Technical Report 85-36, NAGRA, 1985.
[40] R. Pusch, H. Hökmark, L. Börgesson, Outline of models of water and gas flow through smectite clay buffers, SKB Technical Report TR 87-10, SKB, Stockholm, 1987.
[41] T.R. Lineham, A Laboratory study of gas transport through intact clay samples, NIREX report NSS/R155, 1989, 21 p.
[42] S.T. Horseman, J. Harrington, Migration of repository gases in an overconsolidated clay British Geological Survey, Fluid Processes Group, BGS, Keyworth, UK, techical report WE 94/7, 1994.
[43] M.N. Gray, T.L. Kirkham, A.W.L. Wan, J. Graham, On the gas breakthrough resistance of engineered clay barrier. Materials proposed for the nuclear fuel disposal. CNS International Conference on deep Geological Disposal of Radioactive Waste, Winnipeg, Manitoba, Canada, 16–19 September 1996.
[44] K. Tanai, T. Kanno, C. Gallé, in: Proceedings of the MRS'96 Meeting, vol. 465, Boston, USA, December 1996, (1997) p. 995.
[45] R.R. Berg, Am. Assoc. Petroleum Geologists Bull. 59 (1975) 939.
[46] M. Smialowski, Hydrogen in Steel, Pergamon, London, 1962.
[47] P.K. Subramanyan, in: J. Bockris, et al. (Eds.) Comprehensive Tratise of Electrochemistry, vol. 4, Plenum, New York, 1981.
[48] J.M. Gras, l'Hydrogène dans les métaux : techniques de chargement et méthodes d'étude des effets de l'hydrogène dans les matériaux métalliques. Application au cas des aciers et des alliages de nickel, EDF Technical note HT-45/PV G 330-A, 1988.
[49] J. O'M Bockris, M.A. Gershaw, M.A. Fullenwider, Electrochem. Acta 15 (1970) 47.
[50] J. O'M Bockris, P.K. Subramanyan, J. Electrochem. Soc. 118 (1971) 1114.